JOURNAL OF BACTERIOLOGY, Sept. 2004, p. 6168–6178 Vol. 186, No. 18
0021-9193/04/$08.00+0 DOI: 10.1128/JB.186.18.6168–6178.2004


# AglZ Is a Filament-Forming Coiled-Coil Protein Required for Adventurous Gliding Motility of *Myxococcus xanthus*

Ruifeng Yang,[1] Sarah Bartle,[1] Rebecca Otto,[1] Angela Stassinopoulos,[1] Matthew Rogers,[1] Lynda Plamann,[2] and Patricia Hartzell[1]*

*Department of Microbiology, Molecular Biology, and Biochemistry, University of Idaho, Moscow, Idaho,[1] and School of Biological Sciences, Cell Biology and Biophysics, University of Missouri, Kansas City, Missouri[2]*

Received 23 December 2003/Accepted 10 June 2004

**The *aglZ* gene of *Myxococcus xanthus* was identified from a yeast two-hybrid assay in which MglA was used as bait. MglA is a 22-kDa cytoplasmic GTPase required for both adventurous and social gliding motility and sporulation. Genetic studies showed that *aglZ* is part of the A motility system, because disruption or deletion of *aglZ* abolished movement of isolated cells and *aglZ sglK* double mutants were nonmotile. The *aglZ* gene encodes a 153-kDa protein that interacts with purified MglA in vitro. The N terminus of AglZ shows similarity to the receiver domain of two-component response regulator proteins, while the C terminus contains heptad repeats characteristic of coiled-coil proteins, such as myosin. Consistent with this motif, expression of AglZ in *Escherichia coli* resulted in production of striated lattice structures. Similar to the myosin heavy chain, the purified C-terminal coiled-coil domain of AglZ forms filament structures in vitro.**

*Myxococcus xanthus* has a complex life cycle. In the presence of adequate nutrients, the cells undergo vegetative growth and divide, but when the cells are starved of nutrients they aggregate and form fruiting bodies containing myxospores. When nutrients become available, myxospores can germinate into vegetative cells.

Gliding motility of *M. xanthus* requires a solid surface and is controlled by two sets of genes: S (social) genes, which predominantly control movement of groups of cells (47), and A (adventurous) genes, which predominantly control movement of single cells (17). Both S and A motility are involved in vegetative swarming and developmental aggregation. A mutation that inactivates either an A gene or an S gene reduces, but does not abolish, gliding (18). However any combination of $A^-$ and $S^-$ mutations abolishes gliding, revealing that A and S mechanisms of motility are not only different but also independent.

Cells lacking S motility can still move as single cells by using the A system and form colonies with lace-like flares of individual cells at the edges. Various studies have shown that *M. xanthus* social motility requires type IV pili, extracellular matrix fibrils, lipopolysaccharide (LPS), and FrzS, a response regulator–coiled-coil hybrid protein (6, 9, 42, 45). Cells lacking A motility can still move in groups using the S system and form colonies with ruffles of closely grouped cells at their edges. Recent studies have shown that the A motility system may be powered by secretion of a polyelectrolyte through polar nozzle-like structures (46).

The A and S motility systems are adapted for optimal movement in different environments. Mutants with only A motility ($A^+$ $S^-$) glide like the wild-type strain over 1.5% agar surfaces but move more poorly than the wild-type over 0.3% agar. The opposite is true for $A^-$ $S^+$ strains, which move more poorly over 1.5% agar but behave like the wild type on 0.3% agar. When mutant cells are viewed by videomicroscopy, $A^+$ $S^-$ cells can move as single cells, but $A^-$ $S^+$ cells need to be near other cells to move.

Single mutations in only one known *M. xanthus* gene, *mglA*, prevent both A and S motility (16). Colonies formed by *mglA* mutants, like those of $A^-$ $S^-$ double mutants, do not spread and have a sharp edge without ruffles or flares. The *mglA* gene encodes a 22-kDa Ras-like GTPase that is essential for gliding and development, but not for growth (15, 38).

MglA does not appear to be involved directly in the mechanism(s) of gliding. Although colonies formed by *mglA* mutants are indistinguishable from the colonies formed by $A^-$ $S^-$ double mutants, time-lapse studies of individual cells have shown that *mglA* mutants reverse direction 17 times more often than cells of the wild-type strain (2.9/min for Δ*mgl* versus 0.17/min for DK1622) (36). Hence, they are capable of gliding but are incapable of making net movement. *mglA* mutants appear to produce the components, such as pili, fibrils, and polyelectrolyte, that are required for A and S motility (39; R. Otto and P. Hartzell, unpublished data). Hence, the role of MglA may be to coordinate the two gliding motility systems or regulate the frequency with which cells reverse direction while gliding.

If MglA regulates the two motility systems, it is likely to interact with a component of each system to undertake different roles in cell motility. Recently, our investigators showed that MglA interacts with a tyrosine kinase that is required for S motility and development in *M. xanthus* (39). In this study, we report on another protein, AglZ, that interacts with MglA and is required for A motility.

* Corresponding author. Mailing address: Department of Microbiology, Molecular Biology, and Biochemistry, University of Idaho, Moscow, ID 83844. Phone: (208) 885-0572. Fax: (208) 885-6518. E-mail: hartzell@uidaho.edu.

## MATERIALS AND METHODS

**Strains, plasmids, and media.** Strains, plasmids, and oligonucleotides used in this study are listed in Tables 1 and 2. *Escherichia coli* DH10B and JM109 were used for the construction and maintenance of plasmid DNA and for the ampli-

TABLE 1. Bacterial strains and plasmids

| Strain or plasmid | Relevant features and construction | Reference |
|---|---|---|
| *M. xanthus* strains | | |
| DK101 | Leaky $S^-$ gliding; *pilQ* | 41 |
| DK1622 | $A^+$ $S^+$ $Kan^s$; wild type | 41 |
| MxH1104 | $A^-$ $S^+$; *mglA8 masK815* | 39 |
| MxH1139 | $A^+$ $S^-$ $Spr^r$ $Str^r$; *sglK*1252::pGB2 | 43 |
| MxH1777 | $A^-$ $S^+$ $Kan^r$; Δ*aglU* | 44 |
| MxH2223 | $A^-$ $S^+$ $Kan^r$; *aglZ*::pAGS164; electroporation of pAGS164 into DK1622, select $Kan^r$ | This study |
| MxH2224 | $A^-$ $S^-$ (leaky) $Kan^r$; *aglZ*::pAGS164, *pilQ;* electroporation of pAGS164 into DK101, select $Kan^r$ | This study |
| MxH1139 pAGS164 | $A^-$ $S^-$ $Kan^r$ $Spc^r$ $Str^r$; *aglZ*::pAGS164, *sglK*::pGB2; Mx8 lysate from MxH2224 into MxH1139 ($S^-$) | This study |
| MxH1777 pAGS164 | $A^-$ $S^+$ $Kan^s$; *aglZ*::pAGS164, Δ*aglU*; Mx8 lysate from MxH2224 into MxH1777 ($A^-$) | This study |
| MxH2554 | $A^-$ $S^+$ $Kan^r$; pRY4 (Δ*aglZ*); $aglZ^+$ electroporation of pRY4 into DK1622 | This study |
| MxH2265 | $A^-$ $S^+$ $Kan^s$; Δ*aglZ;* exchange of pRY4 from MxH2254 on 2% galactose | This study |
| MxH2274 | $A^+$ $S^+$ $Kan^r$; *aglZ-his6*, pSMB1; electroporation of pSMB1 into DK1622 | This study |
| MxH2275 | $A^+$ $S^+$ $Kan^r$; *aglZ-his6*, pSMB1; electroporation of pSMB1 into MxH2265 | This study |
| *E. coli* strains | | |
| JM109 | F′ *traD36 proA*$^+$*B*$^+$ *lacI*$^q$ Δ(*lacZ*)M15/Δ(*lac-proAB*) *glnV44* el4$^-$ *gyrA96 recA1 relA1 endA1 thi hsdR17* | 50 |
| Top 10F′ | F′[*lacI*$^q$ Tn*10* ($Tet^r$)] *mcrA* Δ(*mrr-hsdRMS-mcrBC*) ϕ80 *lacZ*ΔM15 Δ*lacX74 deoR recA1 araD139* Δ(*ara-leu*) *7697 galU galK rpsL* (*St*$^r$) *endA1 nupG* | Invitrogen |
| BL21(DE3) | $F^-$ *ompT gal [dcm][lon] hsdS*$_B$($r_B^-$ $m_B^-$); an *E. coli* B strain that carries a λ prophage with the T7 RNA polymerase gene for pET expression vectors | Invitrogen |
| *S. cerevisiae* PJ69-4A | *MAT***a** *trp1-901 leu2-3,112 ura3-52 his3-200 gal4*Δ *gal80*Δ *LYS2*::*GAL1-HIS3 GAL2-ADE2 met2*::*GAL7-lacZ* | 22 |
| Plasmids | | |
| pBGS18 | $Kan^r$; cloning vector | 37 |
| pBJ114 | $Kan^s$ *galK;* cloning vector | B. Julien |
| pCR2.1 | $Kan^r$ $Amp^r$; Topo2.1 cloning vector | Invitrogen |
| pGAD-C(x) | GAL4 activation domain, LEU2, $Amp^r$; yeast two-hybrid vector | 22 |
| pGBD-C(x) | GAL4 binding domain, TRP1, $Amp^r$; yeast two-hybrid vector | 22 |
| pGBD-MglA | In-frame GAL4 binding domain-MglA fusion, TRP1, $Amp^r$; EcoRI HindIII *mglA* gene in pGBD-C2 | This study |
| pAGS152 | 784-bp fragment of *aglZ* in pGAD; LEU2, $Amp^r$; clone recovered from the yeast two-hybrid library | This study |
| pAGS160 | DNA upstream and downstream of *aglZ*; SacI fragment from MxH2223, ligated and recovered in *E. coli* DH10B | This study |
| pAGS163 | ≈2-kb sequence upstream and downstream of *aglZ*; SalI-SacI fragment from pAGS160 in pBGS18 | This study |
| pAGS164 | Partial *aglZ* in pBGS18; HindIII-EcoRI fragment from pAGS152 to pBGS18 | This study |
| pMRλ | *aglZ* in 6-kb λ-ZAP clone; plasmid recovered from the λ-ZAP *M. xanthus* library | This study |
| pMR26 | Full-length *aglZ* in pCR 2.1; oligonucleotides 290 and 299 with pMR-λ as template | This study |
| pRY1 | *aglZ* in pCR2.1; oligonucleotides 302 and 303 with pMR26 template | This study |
| pRY3 | Δ*aglZ* in pCR2.1; deletion of 2,659-bp internal NruI fragment | This study |
| pRY4 | Δ*aglZ* in pBJ114; EcoRI fragment from pRY3 into pBJ114 | This study |
| pRY14 | bp 732 to 4188 region of *aglZ* in pCR2.1; oligonucleotides 303 and 335 with wild-type chromosomal DNA | This study |
| pRY15 | bp 732 to 4188 region of *aglZ* in pET24b; BamHI-HindIII fragment from pRY14 into pET24b | This study |
| pSMB1 | *aglZ* in pET24b; BamHI-HindIII fragment from pRY1 into pET24b | This study |

fication of library DNA. *E. coli* cells were grown at 37°C in Luria broth supplemented with ampicillin (100 μg/ml) or kanamycin (40 μg/ml) where applicable. *M. xanthus* strains were grown at 32°C in medium containing 1% Casitone, 10 mM Tris, 1 mM potassium phosphate, and 5 mM $MgSO_4$ (final pH, 7.5; CTPM medium) (43) supplemented with 40 μg of kanamycin/ml where applicable. *M. xanthus* developmental assays were performed on TPM medium. Restriction enzymes were purchased from Gibco BRL, Promega, and New England BioLabs. *Saccharomyces cerevisiae* strain PJ69-4A was grown in yeast extract-peptone-adenine-dextrose and synthetic complete (SC) minus medium. Chemicals were purchased from Sigma-Aldrich.

**Yeast two-hybrid screen.** A library containing chromosomal DNA from *M. xanthus* was prepared in pGAD-C1, pGAD-C2, and pGAD-C3 vectors as described elsewhere (39). Yeast transformations were performed using the quick and easy method (13). For transformations of the library, plasmid DNA (0.1 μg for 1-fold transformation, 1.0 μg for 10-fold transformation) was used to transform yeast using the high-efficiency method (1). Efficiencies were determined on SC minus Leu and Trp and varied from 500,000 to 1,100,000 colonies/μg of DNA. The three different translational reading frames of the library were transformed separately, in triplicate, into PJ69-4A containing pAGS145 (GBD-*mglA*). Colonies that grew on SC minus Leu, Trp, and His were replica plated onto SC minus Leu, Trp, and Ade medium, as described elsewhere (22). Colonies that grew on medium lacking adenine were tested further for β-galactosidase activity. Plasmid DNA was recovered from colonies that satisfied three conditions: (i) growth on SC minus Leu, Trp, and His; (ii) growth on SC minus Leu, Trp, and Ade; and (iii) β-galactosidase activity.

**Recovery of plasmid DNA from yeast.** Colonies that contained the pGAD plasmid and a gene encoding a protein that interacted with pGBD-*mglA* were isolated, and plasmid DNA, named pAGS152, was recovered. The isolated plasmids were electroporated into *E. coli* DH10B cells and selected on Luria broth-ampicillin. Sequence analysis showed that pAGS152 contained a 784-bp insert of *M. xanthus* DNA in pGAD. To confirm the protein-protein interaction, the unknown gene in pGAD was reintroduced along with pGBD-*mglA* into PJ69-4A and plated on SC minus Leu, Trp, His, and Ade. The *M. xanthus* DNA insert in

TABLE 2. Oligonucleotide primers

| Primer | Nucleotide sequence |
|---|---|
| A | 5′ CCC AAG CTT CAT GGA GCG TCG GGT CCT CAT CG 3′ |
| B | 5′ CGG GAT CCG GCT TGT CCA ACT CGTCCAA ACT CGT CCA CCA G 3′ |
| GADF | 5′ GAA GAT ACC CCA CCA AAC 3′ |
| GADR | 5′ CAC GAT GCA CAG TTG AAG 3′ |
| 290 | 5′ CAT ATG GGA TGT TCC GGT TTT CAC AGC ACT 3′ |
| 299 | 5′ GAA TTC CCC TTG TCC AAC TCG TC 3′ |
| 302 | 5′ CCG GGA TCC GAT GGA GCG TCG GGT CCT CAT CG 3′ |
| 303 | 5′ CCC AAG CTT CTT GTC CAA CTC GTC CAC CAG 3′ |
| 319 | 5′ CGA GGA CGA AGA GCC CGA GGA AAT CTC 3′ |
| 320 | 5′ GCC GGA CTG CTC CTT CAG CTC CGC GCG GAG GAC GAC CAG G 3′ |
| 335 | 5′ CGG ATC CGC TCT CCG GCG AGG ACC GCA TC 3′ |

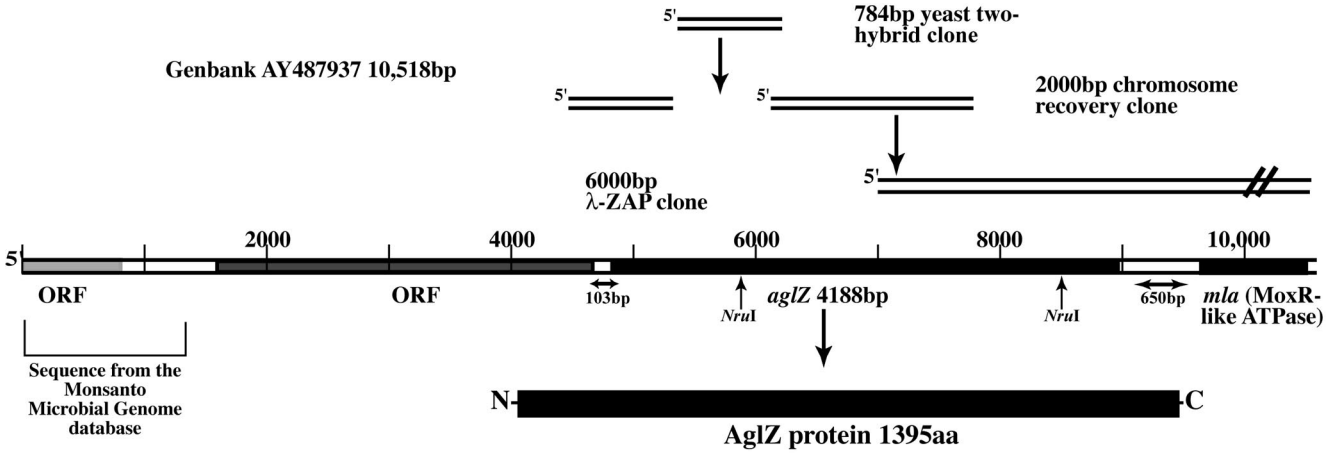


FIG. 1. Cloning of the *aglZ* gene. A 784-bp partial sequence of *aglZ* was recovered from the yeast two-hybrid library and named pAGS152. The 5′ end of the *aglZ* gene and upstream DNA sequence were recovered by matching with contig MYX10C862 from the Monsanto Microbial Genome database of the *M. xanthus* genome. The 3′ end of the *aglZ* gene and the downstream gene were recovered by integration of a partial *aglZ* clone, pAGS164, into the *M. xanthus* chromosome. Chromosomal DNA was digested with SacI to yield pAGS160. The 2-kb fragment subcloned from pAGS160 was used as a probe to identify a 6-kb fragment containing *aglZ* from the λ-ZAP library.

pGAD plasmids, which were confirmed to carry fusions that interact with GBD-MglA, was recovered by PCR using primers GADF and GADR. The PCR product was cloned into pCR2.1 and sequenced. Sequence was obtained using an ABI Prism sequencing apparatus with primers that complemented the forward and reverse regions flanking the insert.

Because the 784-bp insert was recovered from a reaction that used the pGAD-C2 library, we could predict the reading frame for the gene. Based on this, we concluded that the 784-bp fragment was missing the 5′ and 3′ ends of the gene. Sequence upstream of the 784-bp fragment was recovered from the Monsanto Microbial Genome database of the *M. xanthus* genome. The 5′ end of the fragment aligned with the end of the 6,633-bp Monsanto contig MYX10C862, but no match was found for the 3′ end of the fragment.

To obtain sequence downstream of the 784-bp fragment, the scheme shown in Fig. 1 was employed. Plasmid pAGS152 was digested with HindIII and EcoRI to liberate the 784-bp fragment, which was ligated with HindIII- and EcoRI-cut pBGS18 to generate pAGS164. Plasmid pAGS164 was introduced into the chromosome of *M. xanthus* DK1622 (wild type) by electroporation. Of the 78 Kan$^r$ colonies that were isolated, all exhibited an A$^-$ S$^+$ colony phenotype. One representative colony was selected and named *M. xanthus* MxH2223. Genomic DNA was isolated from strain MxH2223 by using the Easy DNA protocol (Invitrogen) and digested with SacI at 37°C for 12 h. The enzyme was heat inactivated at 65°C for 30 min and then dialyzed against 1,000 volumes of distilled water on a 0.025-μm-pore-size filter (Millipore) for 30 min. The DNA was then diluted 1:20, incubated with T4 DNA ligase at 25°C for 12 h, dialyzed, and introduced into *E. coli* DH10B by electroporation. A plasmid, pAGS160, containing about 15 kb of chromosomal DNA flanking the original fragment was recovered from Kan$^r$ colonies. A 2-kb fragment predicted by restriction mapping to contain DNA upstream and downstream of the known sequence was subcloned into pBSG18 to yield pAGS163. pAGS163 was used as probe to recover a larger clone, named pMRλ, from a λ-ZAP library of *M. xanthus* DNA. Plasmid pMRλ contained ≈6,000 bp of sequence downstream of the 784-bp fragment. When compared with the Monsanto Microbial Genome (Cereon) database, we found a match with contig MYX10C1267. The sequences of contig MYX10C862 (partial), pAGS163, pMRλ, and MYX10C1267 (partial sequence) were assembled as a 10,581-bp fragment by using Vector NTI software. The fragment recovered from the original two-hybrid clone corresponded to an internal region of a 4,188-bp gene. Because disruption of this gene abolished A motility, the gene was named *aglZ*. The sequence and predicted products of *aglZ* and flanking regions were analyzed using Frameplot 3.0β (21) and BLAST (2).

**Transductions.** The generalized transducing phage Mx8 was used to transfer the *aglZ* disruption into different genetic backgrounds (27). Phage lysates of *M. xanthus* MxH2224 cells were prepared as described elsewhere (27). Immediately prior to transduction, an aliquot of the phage lysate was irradiated with UV light for 1 min in a UV Stratalinker 1800 (Stratagene) and then mixed with the recipient strain (wild-type and *aglU* and *sglK* mutant strains) for 20 min at 25°C and plated on CTPM supplemented with kanamycin. Plates were incubated for 4 to 6 days at 32°C until colonies arose.

**Construction of an *aglZ* deletion mutation in *M. xanthus*.** Strain MxH2265 was constructed to carry a deletion in the coding region for *aglZ*. Plasmid pMR26 was digested with NruI, which cleaves at bp 5904 and 8563 in AY487937 (bp 1108 and 3767 of *aglZ*), to eliminate a 2,659-bp internal fragment of *aglZ*. The large fragment, containing vector sequence plus 1,107 bp of the 5′ end of *aglZ* and 418 bp of the 3′ end of *aglZ*, was purified and ligated to yield pRY3. The 1.6-kb EcoRI fragment from pRY3 was purified and cloned into EcoRI-digested pBJ114, which carries *galK* and *nptII* genes, to make pRY4. pRY4 was introduced into DK1622 by electroporation, and Kan$^r$ colonies were selected. Recombination of plasmid pRY4, which carries *galK*, *nptII*, and Δ*aglZ*, with chromosomal *aglZ* in the motile strain DK1622 was used to generate a Kan$^r$ merodiploid, MxH2254. MxH2254 was grown on CTPM medium without selection to ≈5 × 10$^8$ cell/ml and then diluted 1:50 in fresh medium every other day for a period of 2 weeks. After >10 generations, 100-μl aliquots were plated on CTPM medium with 2% galactose to promote excision of the integrated plasmid caring *galK* and allele exchange (40). About 30% (121 of 400) of the colonies exhibited a defect in A motility. These colonies were transferred to CTPM plates without antibiotic and incubated at 32°C for 3 days. Chromosomal DNA from four Kan$^s$ A$^-$ S$^+$ colonies was prepared for further analysis. The PCR was performed using oligonucleotide primers A and B (Table 2) to confirm the presence of *aglZ* deletion. Amplification of the *aglZ* gene from the wild-type strain yielded a 4.2-kb product, whereas amplification of the *aglZ* gene from two of the four A$^-$ S$^+$ strains yielded only a 1.6-kb product, showing that 2.6 kb of the *aglZ* fragment had been removed (data not shown). Southern analysis was used to confirm these results (32). Primer 319, which anneals with a region 529 bp upstream of the ATG start in *aglZ*, and primer 320, which anneals with a region 171 bp downstream of the ATG start of *aglZ*, were used in the PCR to make a 700-bp hybridization probe by using the NEBlot Phototope kit (New England BioLabs). Chromosomal DNA from the wild-type parent and A$^-$ mutants, digested with BspEI, confirmed the presence of a 2.66-kb *aglZ* deletion in MxH2265.

**Phenotypic analysis.** The spreading rate was determined by the method of Shi and Zusman (34) as follows. *M. xanthus* strains were grown to a density of 5 × 10$^8$ cells/ml in CTPM medium at 32°C, harvested by centrifugation, and suspended in TPM buffer to 5 × 10$^9$ cells/ml. In triplicate, 5 μl of concentrated cells was spotted onto CTPM plates containing either 1.5 or 0.3% agar, and colony diameters were measured at 24-h intervals.

Time-lapse analysis of cell motility was performed by photographing cells spread on a thin layer of 1.5% CTPM. In each case, roughly 10 μl of a dilute cell suspension (10$^7$ cells/ml) was placed on the thin layer of agar in the middle of the chamber slide. Motility also was assayed for cells treated with methylcellulose, which has been shown to suppress certain motility defect phenotypes (19). Cells on the chamber slide were overlaid with 150 μl of a solution containing 1%

methylcellulose and 0.1% pyruvate. Images were collected at 1-min intervals for 20 min with a Kodak DC-290 digital camera attached to a Nikon FXA labphot-2 microscope and assembled to video using Quicktime 6.0 and NIH Image programs.

The *aglZ* mutant was compared with the wild-type strain to ascertain the presence of cellular components known to be critical for gliding. The production of extracellular fibrils and pili by the Δ*aglZ* mutant was examined by immunoblot analysis using monoclonal antibody 2105, which reacts with the zinc metalloprotease FibA in fibril material (7, 23), and polyclonal antibody against PilA (48), respectively. LPS (O-antigen) and fibrils also were assayed by gel electrophoresis and Congo red binding, respectively, as described elsewhere (3, 9).

Development assays were performed by plating several spots containing $10^7$ cells on TPM starvation agar plates and incubating at 32°C for 120 h (24). After 5 days, the plates were incubated at 50°C for 2 h to destroy vegetative cells, harvested in buffer, and sonicated briefly to break clumps. The number of heat-resistant spores was determined by counting the number of colonies produced after allowing spores to germinate on rich medium (CTPM agar).

**Expression of *aglZ*.** The *aglZ* gene was cloned into the expression vector pET24b to yield an *aglZ-his6* fusion as follows. The *aglZ* gene was amplified from pMR26 with primers 302 and 303, and the ~4.2-kb product was cloned into pCR2.1 to yield pRY1. The *aglZ* gene was removed by digesting pRY1 with BamHI and HindIII and cloned into pET24b to yield pSMB1. The plasmid pSMB1 was subsequently electroporated into the induction host *E. coli* BL21-A1 and into wild-type strain DK1662 and Δ*aglZ* strain MxH2265 to yield MxH2274 and MxH2275, respectively.

Expression of *aglZ* was induced upon addition of isopropyl-β-D-thiogalactopyranoside (IPTG) and arabinose to 1 mM and 1%, respectively, to 200 ml of *E. coli* BL21-A1 cells at an optical density at 600 nm of 0.4. After 3 h, cells were harvested by centrifugation, suspended in 1 ml of 10 mM Tris (pH 7.4), and passed twice through a French pressure cell at 18,000 lb/in$^2$. Cell extract was prepared by centrifuging the lysed material at 20,000 × *g* for 30 min. The supernatant was passed over a Talon resin that had been equilibrated with phosphate-buffered saline (PBS). After washing the column with PBS buffer, AglZ-His was eluted with 150 mM imidazole in PBS buffer. All buffers were at pH 7.

To amplify the coiled-coil region of *aglZ*, primer 335, which anneals with DNA at a site 732 bp downstream from the ATG start in *aglZ*, and primer 303, which anneals with DNA at the 3′ end of *aglZ*, were used in the PCR. The PCR product was cloned into pCR2.1 and subcloned into pET24b to yield pRY15. Expression of this truncated version of *aglZ*, called *aglZ*-coil, in *E. coli* DE3 cells was induced with 1 mM IPTG. The 130-kDa AglZ-coil was purified by the same method used to purify the full-length protein described above.

**Complementation analysis.** To determine if the *aglZ* gene is able to complement the A$^-$ phenotype of strain MxH2265 (Δ*aglZ*), plasmid pSMB1, which carries an *aglZ-his6* fusion, was introduced into MxH2265 by electroporation to make strain MxH2275. Because MxH2265 retains about 1,108 bp of the 5′ end of the chromosomal copy of the *aglZ* gene, homologous recombination can occur between the chromosome and the *aglZ* gene on pSMB1. Transformants were selected on CTPM plates containing 40 μg of kanamycin/ml. Production of AglZ-His was confirmed by immunoblot analysis using anti-His antibody.

**Electron microscopy.** To determine if AglZ might form a structure in vivo, *E. coli* cells expressing AglZ-coil were fixed with 2% (vol/vol) glutaraldehyde and 2% paraformaldehyde in 0.1 M sodium cacodylate buffer (pH 7.2) for 2 h at room temperature and subsequently washed with the same buffer. The samples were then posttreated in 2% (wt/vol) osmium tetroxide overnight at 4°C, dehydrated in acetone, embedded in Spurrs resin (Polyscience), and cut into thin sections using a ultramicrotome.

A sample of purified AglZ-coil was stored at 4°C for several days, during which time a precipitate formed. The precipitate was removed carefully and diluted in distilled water to a protein concentration of about 30 μg/ml. A 3-μl aliquot was applied to carbon-coated grids, left for 1 min, and blotted to near dryness before staining for 1 min with 0.5% uranyl acetate at pH 5.0. All samples were examined using a JEOL JEM-1200 transmission electron microscope operating at an accelerating voltage of 100 keV.

**Immunoblot analysis.** To examine expression of *aglZ-his* in *M. xanthus*, immunoblots of extracts from *M. xanthus* strains MxH2274 and MxH2275 bearing *aglZ-his* fusions were probed with antibody. AglZ-His fusion protein was detected by primary anti-His mouse monoclonal antibody and goat anti-mouse secondary antibody conjugated with horseradish peroxidase (HRP). The samples were developed using the ECL detection kit (Perkin-Elmer) according to the manufacturer's instructions.

**Protein cross-linking.** Protein cross-linking was performed based on the procedures described previously, with modifications (14, 35). A 10-μl aliquot of 3 μM affinity-purified AglZ-His fusion protein and 10 μl of 3.8 μM affinity-purified MglA-His protein were mixed with 1% formaldehyde or 10 mM dimethyl pimelimidate (Pierce). Controls contained 3 μM bovine serum albumin (BSA; Sigma) in place of MglA-His. Following a 60-min incubation at ≈23°C, the samples were mixed with sodium dodecyl sulfate (SDS) sample buffer and separated by SDS–10% polyacrylamide gel electrophoresis (SDS-PAGE). Proteins were transferred to polyvinylidene difluoride membranes and probed with anti-MglA primary antibody and anti-rabbit secondary antibody conjugated with HRP. HRP was assayed as described above.

**Dot-far Western blotting analysis.** The dot-far Western blotting method of Ohba et al. (30) was performed with the following modifications. Aliquots containing 3 and 6 pmol of purified MglA-His fusion protein (or BSA for controls) were absorbed to nitrocellulose. A small amount of AglZ-His fusion protein (0.3 pmol) was also spotted on the membrane as a positive control. When the samples were dry, the membrane was blocked for 1 h at 23°C with 5% (wt/vol) skim milk, washed in PBS-T (10 mM Na-$PO_4$, 150 mM NaCl, 0.05% Tween 20; pH 7.5), and then incubated with 2 ml of PBS-T containing 1.5 μM AglZ-His fusion protein at 23°C for 1 h. The membrane was washed three times with PBS-T and probed with anti-AglZ diluted 1:10,000 in 5% skim milk–PBS buffer for 1 h at 23°C. After washing three times with PBS, the membrane was probed with anti-rabbit secondary antibody conjugated with HRP and developed as described above.

**Nucleotide sequence accession number.** The 10,581-bp sequence of the *aglZ* gene and flanking DNA has been deposited in GenBank as accession number AY487937.

## RESULTS

**Isolation of the *aglZ* gene, which encodes a protein that interacts with MglA.** To find proteins that interact with MglA, *mglA* was fused with the GAL4 binding domain to generate a translational fusion and used as bait with a pGAD library containing random fragments from *M. xanthus* in the yeast two-hybrid system. Yeast that carried GBD-MglA and an interacting clone from the GAD-C2 library expressing GAD-X were identified as colonies that grew on medium lacking histidine and adenine in a strain engineered to express *HIS* and *ADE* from *GAL4* promoters. Plasmids pGAD-X and pGBD-*mglA* were isolated from yeast and recovered in *E. coli*. Plasmids pGAD-X and pGBD-*mglA* were used to retransform a naïve PJ69-4A yeast host together and with controls pGBD and pGAD, respectively. Growth on medium lacking His or Ade occurred only when GAD-X was paired with GBD-*mglA*. Plasmid pGAD-X was named pAGS152. Confirmation of the interaction was shown by assaying the reciprocal pair of plasmids. Yeast cells carrying pGAD-*mglA* and pGBD-X grew on medium lacking adenine, whereas cells with pGAD-*mglA* plus pGBD or pGAD plus pGBD-X failed to grow.

The sequence of pAGS152 contained a 784-bp insert, but the gene that was in frame with GAD lacked an apparent stop codon. To recover additional sequence, the scheme shown in Fig. 1 was employed. A derivative of pAGS152, pAGS164, was introduced into *M. xanthus* and integrated onto the chromosome. Yellow, Kan$^r$ colonies carrying pAGS164 exhibited S motility, but not A motility (Fig. 2C), suggesting that the gene recovered from the yeast two-hybrid is part of the A motility system. Hence, the name *aglZ* (for adventurous gliding Z) was assigned to this gene. Sequence analysis of plasmid pAGS163, which carries sequence flanking the pAGS164 chromosomal insertion, yielded the 5′ end of the *aglZ* gene and additional sequence downstream but appeared to lack the 3′ end of the gene. To obtain the 3′ end of *aglZ*, a 2-kb fragment of *aglZ* from pAGS163 was used as probe to isolate pMRλ from an *M. xanthus* λ-ZAP library. Sequence analysis of pMR26, which was subcloned from pMRλ, yielded the 3′ end of *aglZ*. Contigs

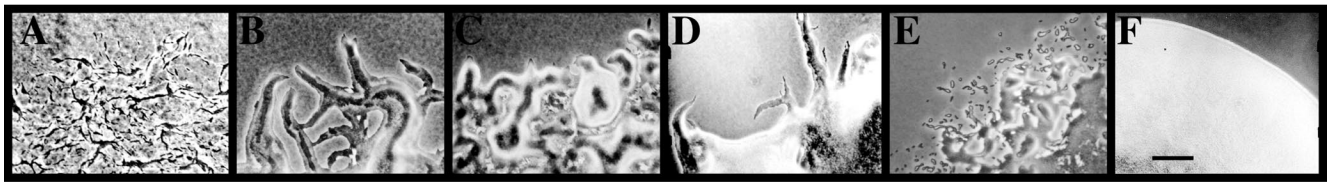


FIG. 2. Phenotypes of double mutants confirmed that *aglZ* is part of the A motility system. Double mutants were constructed as described in Materials and Methods. (A) DK1622 (wild type); (B) MxH1777 (Δ*aglU*); (C) MxH2223 (*aglZ*::pAGS164); (D) MxH1777 pAGS164 (*aglZ*::pAGS164 Δ*aglU*); (E) MxH1139 (*sglK*::pGB2); (F) MxH1139 pAGS164 (*aglZ*::pAGS164 *sglK*::pGB2).

MYX10C862 and MYX10C1267 from the Cereon Microbial Genome database (Monsanto) each aligned with a part of the sequence. The assembled sequence has been deposited in GenBank.

***aglZ* is essential for A gliding.** To confirm that *aglZ* is a gene of the A motility system, the *aglZ* disruption in MxH2224 was transduced into strains that carry mutations in known A and S motility genes and the phenotypes of double mutants were analyzed. As shown in Fig. 2D, the *aglZ aglU* double mutant had an $A^- S^+$ gliding phenotype like that of its *aglU* parent, whereas the *aglZ sglK* double mutant, MxH1139 pAGS164, had an $A^- S^-$ (nonmotile) gliding phenotype (Fig. 2F). These results confirmed that *aglZ* is part of the A motility system.

Because of concern that the phenotype might reflect polar effects on downstream genes due to the integration of pAGS164, a strain carrying a markerless deletion of *aglZ* was made. Recovered colonies exhibited either a normal or a small-colony phenotype. DNA from two colonies with the small-colony phenotype was used as template in the PCR and for Southern analysis to confirm the presence of the engineered *aglZ* deletion and the absence of the parental copy of *aglZ*. Southern analysis revealed bands at 2.3 and 6.5 kb, which hybridized with the probe in the wild-type strain (DK1622), and bands at 2.3 and 3.9 kb in the deletion mutant, which subsequently was named MxH2265. These data showed that MxH2265 is a null mutant for *aglZ*.

The colony phenotype of the MxH2265 mutant was identical with that of strain MxH2223, which carries an insertion in *aglZ* in the wild-type background. These data suggested that the loss of A motility is not due to an effect on genes downstream of *aglZ*. Furthermore, there is a 650-bp gap between the 3′ end of *aglZ* and the next gene, making the notion of a second gene in the operon unlikely. Strain MxH2265 was used for more detailed motility and complementation assays.

Although the *aglZ* mutant possessed S motility, as evidenced by the groups of motile cells at the edge of the colony shown in Fig. 3B, the mutant showed defects in spreading on both 0.3 and 1.5% agar surfaces (Fig. 3D). This was surprising, because mutants that lack A motility typically show reduced spreading on 1.5% agar but are able to spread on 0.3% agar, as S motility is functional under these conditions. The motility defect of Δ*aglZ* was characterized further by time-lapse video microscopy. During a 30-min period, isolated cells of the wild-type parental strain DK1622 moved two to three cell lengths (about 25 to 30 μm) in the same direction. In contrast, isolated cells of the Δ*aglZ* mutant MxH2265 did not show any movement under these conditions, even on 1% methylcellulose. Hence, although *aglZ* is essential for A motility, loss of *aglZ* also reduces motility on soft agar, where S motility predominates.

To determine if disruption of *aglZ* alters the production of components known to be required for S motility, extracts of wild-type and mutant cells were assayed for PilA and FibA, indicators of pili and fibrils, respectively. Wild-type and Δ*aglZ* cells have similar amounts of the 27-kDa PilA in whole-cell extracts and in sheared pilus preparations (data not shown). In contrast, Δ*aglZ* cells produce an elevated amount of FibA in the whole-cell extract compared to the wild type. Profiles of the *aglZ* mutant resembled those of the wild-type strain on acrylamide gel assays (for O-antigen, LPS) and Congo red binding for fibril material (data not shown). The slight increase in FibA may account for the reduced capacity for movement on soft (0.3%) agar.

The Δ*aglZ* mutant (MxH2265) was assayed for developmental defects in nutrient-free TPM agar plates as described in

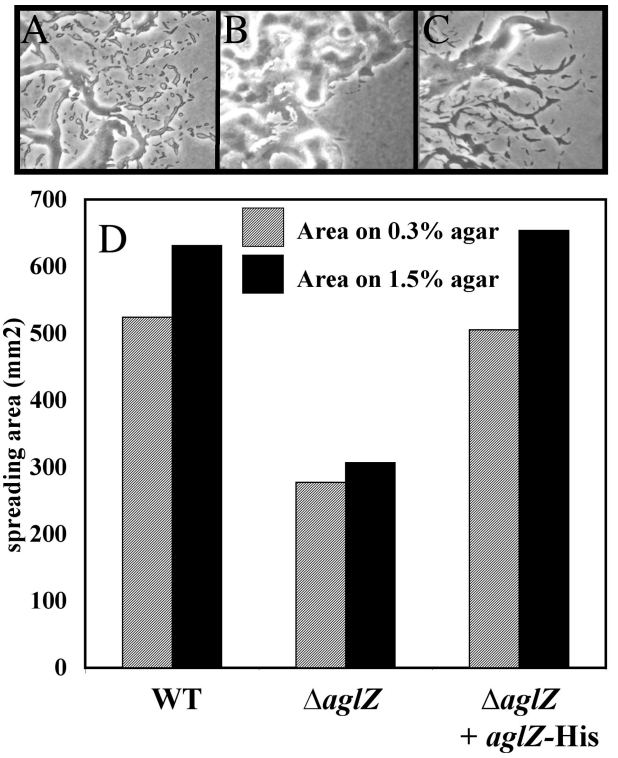


FIG. 3. Mutation in the *aglZ* gene blocks A motility. (A) Edge of a wild-type (DK1622) colony; (B) edge of a Δ*aglZ* (MxH2265) colony; (C) edge of a colony of the mutant complemented with *aglZ-his* (MxH2275). Images were captured using a Nikon Microphot-FXA microscope at 20× magnification. (D) Colony spreading areas on 0.3 and 1.5% agar after 96 h.

Materials and Methods. The mutant strain produced dark fruiting bodies similar to those of the wild-type strain. After 5 days, spore samples were heated at 50°C for 2 h and then transferred to CTPM rich medium plates to stimulate the germination of heat-resistant spores. The Δ*aglZ* mutant produced a wild-type complement of heat-resistant spores.

**The motility defect of Δ*aglZ* can be complemented by an *aglZ-his6* fusion.** The plasmid pSMB1, which carries *aglZ-his6*, was electroporated into the *M. xanthus* MxH2265 (Δ*aglZ*) mutant strain, and Kan$^r$ colonies were selected to yield MxH2275. Plasmid pSMB1 contains only the *aglZ* gene and can integrate onto the chromosome by homologous recombination with the 5′ end of Δ*aglZ* or the 3′ end of the Δ*aglZ* gene on the chromosome. Only recombination between the 5′ end of Δ*aglZ* and the plasmid-borne *aglZ* could generate a functional copy of *aglZ* with its promoter. Since a larger portion of the 5′ region of *aglZ* remains on the chromosome than the 3′ end, we anticipated that a greater number of recombinants would result from recombination with the 5′ end of *aglZ*. Consistent with this, two different motility phenotypes were found among the Kan$^r$ colonies derived from electroporation of pSMB1 into the Δ*aglZ* mutant. Forty-nine of the 74 transformants produced colonies that were identical to the fully motile wild-type strain, and the remaining transformants were similar to the Δ*aglZ* parent. Motility and development assays of the fully motile transformants were performed alongside the wild-type strain and the Δ*aglZ* parent. As shown in Fig. 3C, numerous single cells could be seen emanating from the edge of the colony, in contrast with the Δ*aglZ* parent in Fig. 3B, which was devoid of single cells. Hence, the *aglZ-his6* fusion complemented the A motility defect of the Δ*aglZ* mutant. Moreover, as shown in Fig. 3D, the ability of MxH2275 to spread on 0.3 and 1.5% CTPM motility agar surfaces was identical to that of the wild type.

***aglZ* encodes a protein related to type 2 myosin.** The deduced *aglZ* gene product, AglZ, is predicted to be a 1,395-amino-acid protein with an expected molecular weight of about 153,600. The N-terminal ≈120 amino acids contain residues that match the consensus for the REC signal receiver domain family (cd00156; 9e−11) of proteins that includes FrzS, CheY, and OmpR (Fig. 4C). FrzS, like AglZ, is a protein required for motility of *M. xanthus* (42). The strongest match was between AglZ and PhoB of *Vibrio cholera* (AAC25063.1). The N termini of these two proteins share 34% identity and 49% similarity (4e−07). AglZ lacks the Asp53 residue that typically is the site of phosphorylation in response regulators. However, like *Mycobacterium tuberculosis* response regulator MprA (52), the aspartate residue at position 48 of AglZ may be a target for phosphorylation.

Following the N-terminal response regulator domain is a 120-residue proline-rich (15 proline residues of 120) linker domain. The isoelectric point for this proline-rich region is predicted to be 10, while the regions before and after this region have a pI of about 4.5. The linker precedes a 1,048-amino-acid domain that is devoid of proline residues. Analysis of this region using the algorithm MULTICOIL (45) indicated a strong tendency to form a coiled-coil structure, with a propensity for dimer formation (Fig. 4D). As shown in Fig. 4B, the predicted coil structures extended over greater than 80% of the protein. This domain included multiple matches with the myosin class II heavy chain (KOG0161; 1e−11).

The *aglZ* fragment originally recovered from the yeast two-hybrid clone encodes a part of AglZ that corresponds to these two domains. When translated, the two-hybrid fragment yielded 193 amino acids, of which ≈73 residues overlapped with the proline-rich region and ≈120 residues overlapped with the beginning of the coiled-coil region.

A comparison of the translated 1,395-amino-acid sequence of *aglZ* with known proteins using BLAST (2) revealed 21% identity and 43% similarity with 467 residues of myosin heavy chain isoform A of *Loligo pealei* (AAC24207.1) and 27% identity and 49% similarity with 226 residues of myosin heavy chain, nonmuscle type A (MYH9_Human) of *Homo sapiens*. Although most matches (≥85%) were with myosin proteins, AglZ also shared some identity with the 170-kDa Golgi peripheral membrane protein. These proteins share a common structural motif that enables them to form coiled-coil structures, and many of them play essential roles in cytoskeleton structure and motility.

Coiled-coil proteins are a mixture of hydrophobic and hydrophilic residues repeated every seven amino acids, forming parallel α-helices that intertwine (12). A minimum of four heptad repeats yields a stable coiled-coil structure (29, 31). Amino acids 248 to 1292 of AglZ, which form the coiled-coil domain, contain the requisite heptad repeats (a, b, c, d, e, f, g)$_n$. The sequence showed both four- and seven-heptad repeats. In each heptad, amino acids at positions a and d are comprised of mainly hydrophobic residues, such as leucine, whereas amino acids at positions e and g are comprised mainly of hydrophilic residues, such as glutamate (12). The coiled-coil domain of AglZ also contains 21 repetitive structures that range in size from 5 to 33 amino acid repeats. While the significance of these repeats is not understood, similar patterns of repeats are found in proteins such as fibronectin. Immediately following the coiled-coil domain is a second proline-rich (15% proline) domain. In contrast with the linker domain, the terminal proline-rich tail has a pI of 4.7.

Coiled-coil proteins typically migrate more slowly than expected from their primary sequence predictions. As shown in Fig. 5A, lane 2, two high-molecular-mass bands were detected when full-length AglZ-His6 was expressed in *E. coli* BL21-A1. In contrast, these bands were missing in the uninduced *E. coli* sample and the *E. coli* strain carrying the parent plasmid, pET24b (data not shown). Two protein bands also were detected in *M. xanthus* cells expressing AglZ-His (Fig. 5A, lane 3). The AglZ proteins in *M. xanthus* migrated more slowly than the AglZ proteins in *E. coli*, which hinted that AglZ is modified in *M. xanthus*.

**The C-terminal domain of AglZ forms a structure with a striated pattern in *E. coli*.** In extracts of *E. coli* bearing pRY15, the truncated version of AglZ-His, which lacks the N-terminal response regulator domain, two high-molecular-weight protein bands were seen on Coomassie-stained gels. As shown in Fig. 5B, both bands were greater than the 220-kDa standard, indicating that AglZ-coil forms a structure that is significantly larger than its predicted size (≈130 kDa). This aberrant shift in mobility under denaturing conditions was consistent with proteins that can adopt a coiled-coil structure. FrzS, an *M. xanthus* protein with a domain structure similar to that of AglZ, also

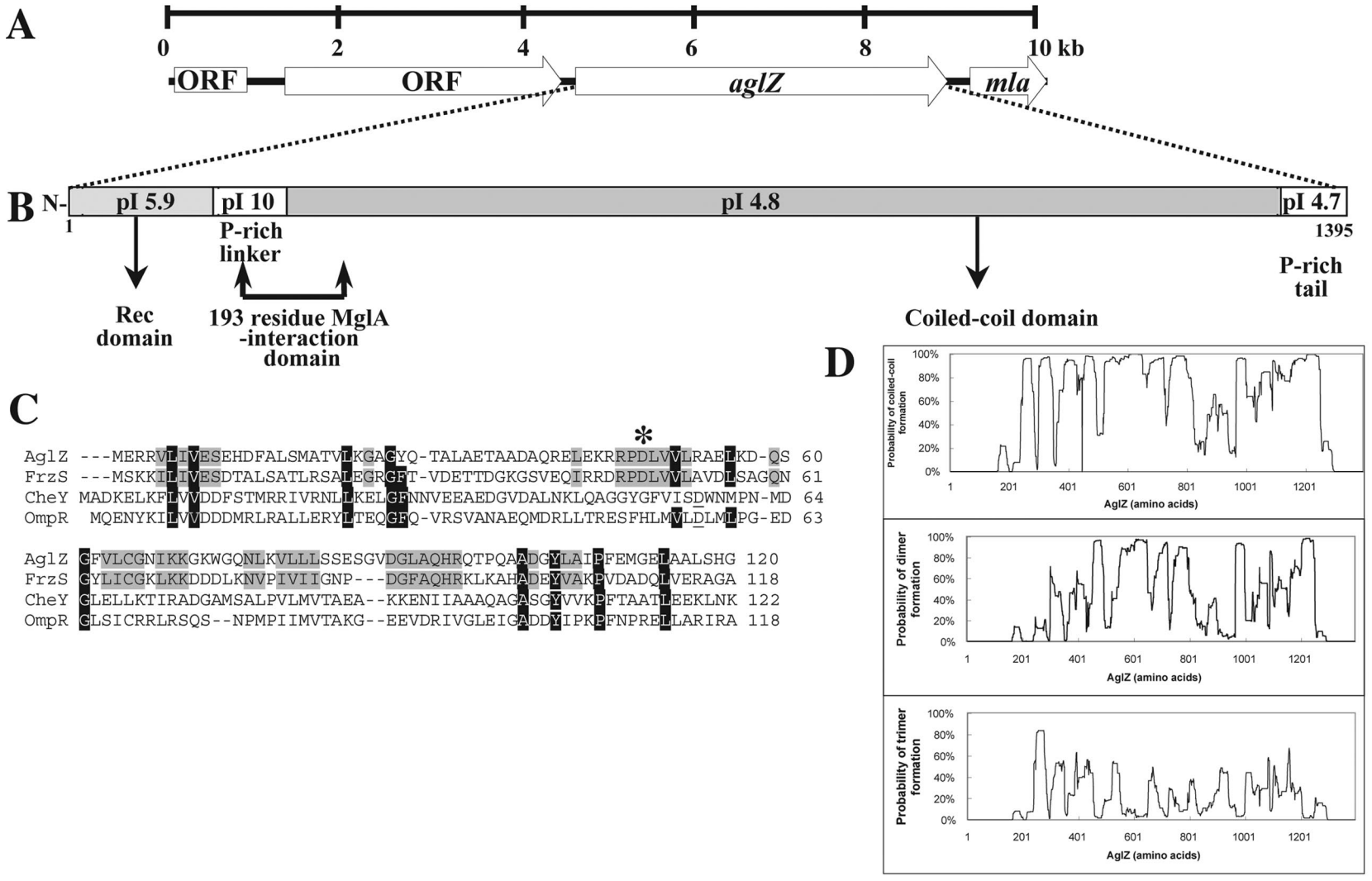


FIG. 4. Domain organization and sequence alignment of AglZ with related proteins. (A) The *aglZ* gene appears to be a single gene operon. (B) AglZ can be divided into four regions based on pI and sequence identity: an N-terminal receiver (Rec) domain is followed by a proline-rich (P-rich) linker separating the Rec domain from the extensive coiled-coil domain. A short, C-terminal proline-rich region follows the coiled-coil domain. (C) Alignment between the N-terminal 120 residues of AglZ and the receiver domain of FrsZ from *M. xanthus* (42) and CheY and OmpR from *E. coli* (28, 49). Identical residues are boxed in black; grey boxes show similar or identical residues for AglZ and FrzS. Asp48, marked by an asterisk, in AglZ may be a target for phosphorylation. Asp53, the residue phosphorylated in most response regulators, is underlined in CheY and OmpR. (D) Output from the coiled-coil prediction program Multicoil (45) shows the probability of coiled-coil formation in the C-terminal domain of AglZ in the top panel. The middle and lower panels show the probability of coiled-coil dimer and trimer formation, respectively.

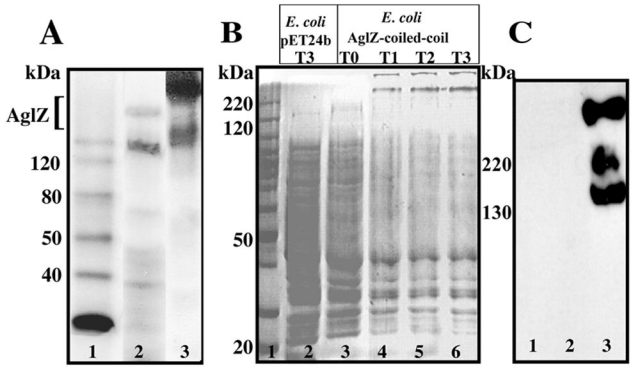


FIG. 5. Expression of AglZ. (A) Immunoblots of whole-cell extracts from *E. coli* pSMB1 and *M. xanthus* MxH2274 were probed with anti-His antibody. Lane 1, protein standards; lane 2, AglZ-His in *E. coli*; lane C, AglZ-His in *M. xanthus*. The bracket marks the position of multiple AglZ bands. (B) Expression of the coiled-coil domain of AglZ revealed two discrete bands at a mass greater than that predicted for AglZ (130 kDa). Lane 1, standards; lane 2, *E. coli* pET24b control 3 h after induction with IPTG; lanes 3 to 6, *E. coli* pRY15 at $t = 0$, 1, 2, and 3 h after induction with IPTG, respectively. (C) Samples shown in panel B (lanes 3 and 6) were probed with anti-His antibody to confirm that the high-molecular-mass species were AglZ-His. Lane 1, protein standards; lane 2, *E. coli* pRY15, uninduced; lane 3, *E. coli* pRY15, induced. Three discrete bands correspond to AglZ-His and multimers of AglZ-His.

shows aberrant migration on SDS-PAGE (42). To confirm that these high-molecular-weight proteins were forms of AglZ, extracts were probed with anti-His6 antibody. Immunoblotting confirmed that the two large bands were forms of AglZ and revealed the presence of a third smaller band estimated to be about 150 kDa (Fig. 5C). The higher-molecular-weight bands were discrete and their sizes were consistent with dimer and trimer forms of AglZ, which can remain associated under SDS-PAGE denaturing conditions but not in the presence of urea (data not shown).

Analysis of cells of *E. coli* producing AglZ-coil by transmission electron microscopy revealed a repeating pattern in the cells due to formation of a higher-order structure (Fig. 6B). This pattern was not present in the induced cells containing only the expression vector pET24b (Fig. 6A). As rod regions of known coiled-coil proteins are predicted to extend 15 nm per 100 amino acids (8), the theoretical length of AglZ-coil (1,045 residues with a 102-residue tail) is expected to be approximately 157 nm. Measurement of the repeating pattern formed by AglZ-coil showed a periodicity of 74 nm (Fig. 6C), which is about half of the length predicted for AglZ-coil. This is in contrast with previous reports for other proteins that form

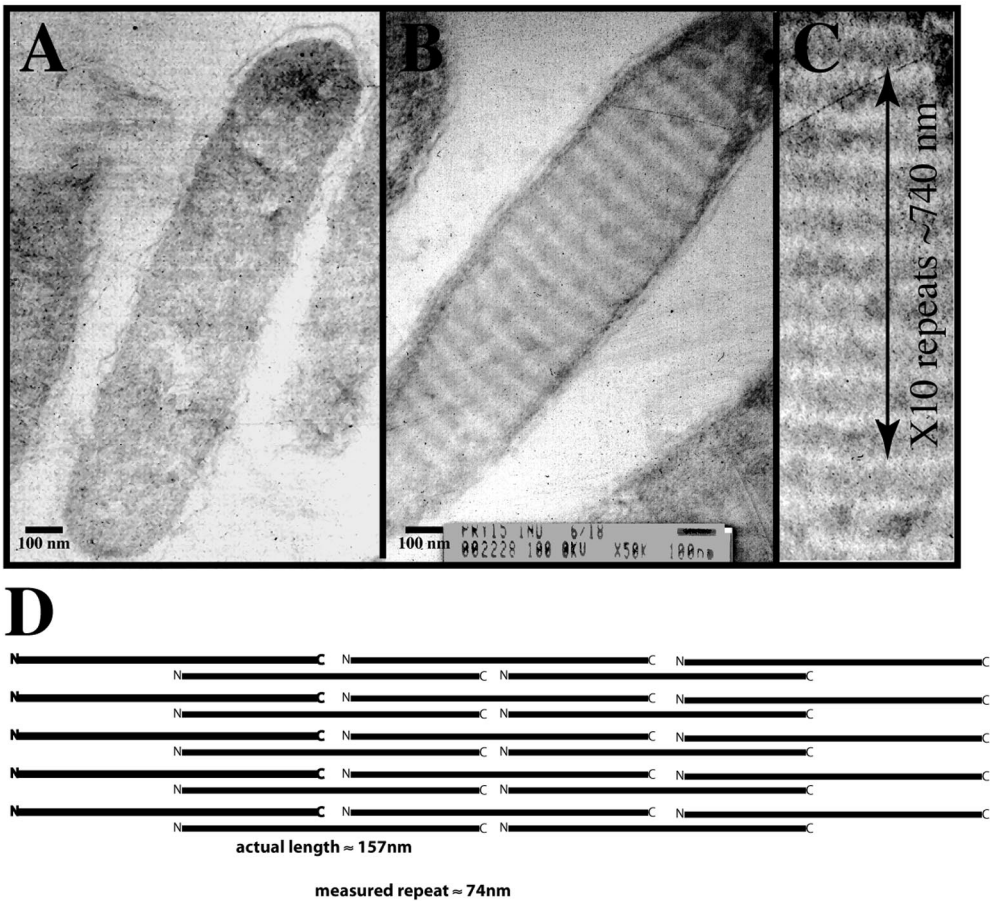


FIG. 6. AglZ forms a structure with a regular repeat when expressed in *E. coli*. (A and B) Electron micrographs of thin-sectioned *E. coli* cells harboring pET24b (A) or pRY15 (B), harvested 3 h after induction with 1 mM IPTG. Photographs were taken at a ×20,000 magnification. (C) The striated pattern produced by overexpression of the C terminus of AglZ repeats every 74 nm. (D) The repeat of the striation is smaller than the size predicted for AglZ as described in the text. This suggests that the overlap between molecules of AglZ extends over a significant region of the protein.

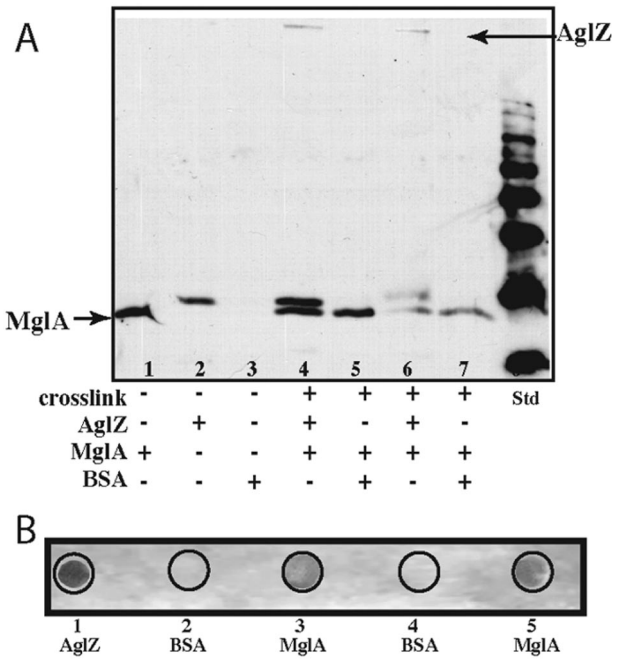


FIG. 7. AglZ interacts with MglA in vitro. (A) AglZ and BSA control protein (3 μM) were mixed with 3.8 μM MglA and incubated in the presence of 10 mM dimethyl pimelimidate (lanes 4 and 5) and 1% formaldehyde (lanes 6 and 7). Reaction products were separated by SDS–10% PAGE, and Western blotting was performed by probing with anti-MglA. In the absence of cross-linker (lanes 1 to 3), no high-molecular-mass MglA was detected. In the presence of cross-linker (lanes 4 to 7), anti-MglA reacted with a high-molecular-mass species that required addition of AglZ to the mixture. (B) Dot-far Western blotting of AglZ-His and MglA-His fusion protein and of BSA with AglZ-His fusion protein as a probe. AglZ (0.3 pmol), 3 pmol of MglA and BSA (spots 2 and 3), and 6 pmol of MglA and BSA (spots 4 and 5) were applied to nitrocellulose membranes and incubated with 1.5 mM AglZ-His fusion protein for 1 h. Samples were then probed with anti-AglZ and HRP-conjugated anti-rabbit antibody with PBS-T washes between each step. In controls lacking the AglZ-His incubation step, only spot 1 (AglZ-His) reacted with the antibody. A small-molecular-mass protein from *E. coli* copurified with AglZ but did not cross-link with AglZ.

striated lattice structures, in which the theoretical periodicity is close to the actual periodicity of the coiled-coil region (20). We interpret this to mean that the light and dark patterns formed by AglZ are caused by the substantial overlap between AglZ molecules, as shown in Fig. 6D.

**Biochemical evidence that AglZ interacts with MglA.** With purified proteins and antibodies in hand, we were able to use more refined methods to confirm the interaction between MglA and AglZ that was predicted from the yeast two-hybrid results. Two biochemical approaches were taken to probe the protein-protein interactions. First, mixtures of purified AglZ and MglA or control protein were treated with various cross-linking agents and then separated on denaturing gels. The proteins were transferred to polyvinylidene difluoride and probed with anti-MglA antibody. As shown in Fig. 7A, antibody reacted with the high-molecular-weight species only in samples that contained MglA, AglZ, and cross-linker. Anti-MglA did not react with AglZ in samples that lacked MglA. Second, the dot-far Western technique (30) was performed. Different amounts of MglA-His, AglZ-His, and BSA were spotted onto nitrocellulose membranes and incubated with and without AglZ. Samples were washed and probed with anti-AglZ antibody and secondary antibody. As shown in Fig. 7B, AglZ selectively bound to different amounts of MglA (areas 3 and 5) and to itself (area 1), but not to BSA (areas 2 and 4).

**AglZ forms a filament structure in vitro.** The formation of striated patterned structures in *E. coli* was reminiscent of striated muscle, and the similarities between AglZ and myosin hinted that AglZ might form a filament structure. To test this idea, AglZ and AglZ-coil were purified to apparent homogeneity and incubated at 4°C. In both samples, a precipitate could be seen after several days. An aliquot of each precipitate was diluted in distilled water, stained with uranyl acetate, and placed on grids. As shown in Fig. 8, electron microscopy revealed the presence of 1- to 3-μm-long filaments having an average diameter of ≈50 nm. Upon close examination, some of the filaments appeared to be hollow, suggesting that the helices of AglZ can rope together by multiple interactions. Filament structures were not detected in the sample prepared from the full-length AglZ protein.

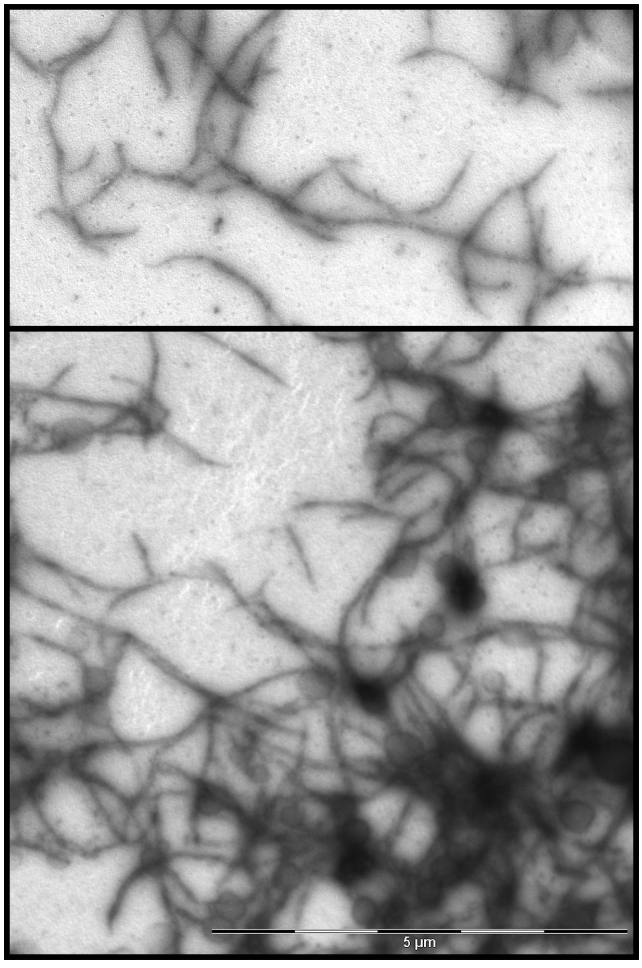


FIG. 8. The AglZ-coil domain forms filaments with a diameter of 50 to 100 nm in vitro. Electron micrographs of isolated AglZ-coil were negatively stained with 0.5% uranyl acetate (pH 5.0).

## DISCUSSION

*M. xanthus* uses two distinct processes to gliding over surfaces. One process, known as S gliding, involves extension and retraction of pili that emanate from one pole of the cell. Mutations that affect the genes for type IV pili (48), the exopolysaccharide-protein matrix that constitutes fibrils (6, 22), and the O-antigen of LPS (9) abolish S motility. The other gliding process is called A motility. Secretion of a polyelectrolyte through polar nozzles is postulated to be the driving force for A motility (46). In support of this idea, genetic studies have shown that two sets of proteins related to the *E. coli* TolABQR proteins are required for A motility (44, 51). In *E. coli*, the Tol proteins form a complex that links the inner and outer membranes and facilitates transport of macromolecules (25). The *M. xanthus* Tol counterparts may be functionally analogous, which makes them prime candidates for the nozzle structure.

The *aglZ* mutants showed a primary defect in A motility, as demonstrated by the lack of isolated cells at the colony edge and reduced spreading on a hard agar (1.5%) surface. When viewed by time-lapse videomicroscopy, Δ*aglZ* showed no single-cell movement on 1.5% agar or on 1% methylcellulose, which can suppress the nonmotile phenotype of particular mutants. Genetically, *aglZ* is part of the A motility system, because when paired with a mutation in an S motility gene, the resulting double mutant was nonmotile.

The *aglZ* mutant exhibited a phenotype that was more severe than most A motility mutants. The mutant showed reduced spreading on soft (0.3%) agar even though flares, or groupings, of cells that are characteristic of S motility were visible at the colony edge, and the mutant appeared to make components necessary for S gliding. Despite the fact that the *aglZ* mutation affected motility, fruiting body development and spore formation were unaffected in the mutant.

The *aglZ* gene appears to be a single gene operon. This is supported by the fact that a disruption mutant has the same phenotype as the deletion mutant, which argues against a polar effect on a downstream gene. Moreover, there is a 103-bp gap between *aglZ* and its upstream gene and a 650-bp gap between *aglZ* and its downstream gene.

The domain organization of AglZ is very similar to that of another *M. xanthus* protein, FrzS, which is required for S motility (42). Both AglZ and FrzS have a large C-terminal coiled-coil domain that is similar to myosin, although the two proteins do not show any significant identity with one another in this region by direct comparison. In place of the N-terminal ATPase head of myosin, these bacterial counterparts have an N-terminal response regulator domain. The N-terminal domain lacks the conserved aspartate at position 53 that is a potential target for modification, but it has an aspartate at position 48 which may be phosphorylated. If phosphorylation of AglZ occurs, it might furnish a primitive regulatory equivalent to ATP hydrolysis in myosin.

The *aglZ* gene first was identified from a clone recovered from the yeast two-hybrid system because it produced a fusion with the GAL4 activation domain that could interact with a binding domain fused with MglA. MglA is a small GTPase that is required for both A and S motility. Previously, our group had shown by suppressor analysis and the yeast two-hybrid assay that MglA interacts with MasK, a membrane-bound tyrosine kinase (39). A mutation in *masK* suppressed a mutation in *mglA* to restore S motility to the *mglA* mutant. The MasK study showed that MglA interacts with a component of the S gliding system. The data presented in this paper confirm that MglA also interacts with a protein that is part of the A motility system. Establishing a link between MglA, AglZ, and MasK is a major step toward understanding how MglA might regulate the two gliding systems. The ability of MglA to interact with a component of each motility system might provide a switch that enables A and S gliding systems to operate simultaneously in the wild-type strain. Because AglZ and MasK are both potential targets for regulation by phosphorylation, it is conceivable that a change in the phosphorylation state of either AglZ or MasK could alter their interaction with MglA. The putative target for phosphorylation in AglZ is in the N-terminal domain near the proline-rich linker region to which MglA binds.

Although the discovery of an interaction between a small GTPase and a myosin-like protein has not previously been reported in a prokaryote, it is well documented in eukaryotic systems. For example, the GTPase Rab6 interacts with the coiled-coil region of several golgins, which are involved in vesicular transport (5), and Ras3A interacts with the coiled-coil domain of Rabin3 (10). Sec4b interacts with the coiled-coil domain of Sec2b, which is essential for vesicular transport in *S. cerevisiae* (4). In these cases, GTPases interact with coiled-coil proteins to transport intermediates. If AglZ functions in an analogous fashion, it may participate in transporting substances that are involved in gliding, subject to regulation by the GTPase MglA.

The finding that AglZ is a filament-forming protein that is structurally related to myosin raises the possibility that the mechanism of A motility is functionally related to myosin-mediated movement. If so, A gliding is more complex than previously thought, and secretion of material through a nozzle as described by Wolgemuth et al. (46) may be only part of the A gliding mechanism. There are numerous historical accounts of filaments in *M. xanthus* that are thought to be involved in movement. AglZ may form the 12-nm filament structures that were described in *M. xanthus* 25 years ago (11). Tubules that were estimated to be ≈13 to 17 nm in diameter were found in the debris of disrupted cells, and 7.5- to 10-nm filaments arranged in a herringbone pattern were described previously (11). Reports of tubules that traverse the length of the cells also have been described (26, 33). Work is under way to ascertain if the filaments described by these three different groups are related to the A motility protein AglZ.

## ACKNOWLEDGMENTS

We thank Christine Davitt at WSU for expert help with electron microscopy and Ann Norton for help with microscopy used for motility analysis.

This work was supported by grant MCB0242191 from the National Science Foundation (NSF), NIH-Idaho BRIN to P.L.H., and NSF REU 0245188 to R.O.

## REFERENCES

1. **Agatep, R., R. D. Kirkpatrick, D. L. Parchaliuk, R. A. Woods, and R. D. Gietz.** 1998. Transformation of *Saccharomyces cerevisiae* by the lithium acetate/single-stranded carrier DNA/polyethylene glycol (LiAc/ss-DNA/PEG) protocol. Tech. Tips Online [Online.] http://www.umanitoba.ca/faculties/medicine/biochem/gietz/2HS.html.
2. **Altschul, S. F., W. Gish, W. Miller, E. W. Myers, and D. J. Lipman.** 1990. Basic local alignment search tool. J. Mol. Biol. **215:**403–410.
3. **Arnold, J. W., and L. J. Shimkets.** 1988. Inhibition of cell-cell interactions in *Myxococcus xanthus* by Congo red. J. Bacteriol. **170:**5765–5770.

4. **Autret, S., R. Nair, and J. Errington.** 2001. Genetic analysis of the chromosome segregation protein Spo0J of *Bacillus subtilis*: evidence for separate domains involved in DNA binding and interactions with Soj protein. Mol. Microbiol. **41:**743–755.
5. **Barr, F. A.** 1999. A novel Rab6-interacting domain defines a family of Golgi-targeted coiled-coil proteins. Curr. Biol. **9:**381–384.
6. **Behmlander, R. M., and M. Dworkin.** 1991. Extracellular fibrils and contact-mediated cell interactions in *Myxococcus xanthus*. J. Bacteriol. **173:**7810–7821.
7. **Behmlander, R. M., and M. Dworkin.** 1994. Integral proteins of the extracellular matrix fibrils of *Myxococcus xanthus*. J. Bacteriol. **176:**6304–6311.
8. **Bourne, H. R.** 1991. Colon cancer. Consider the coiled coil. Nature **351:** 188–190.
9. **Bowden, M. G., and H. B. Kaplan.** 1998. The *Myxococcus xanthus* lipopolysaccharide O-antigen is required for social motility and multicellular development. Mol. Microbiol. **30:**275–284.
10. **Brondyk, W. H., C. J. McKiernan, K. A. Fortner, P. Stabila, R. W. Holz, and I. G. Macara.** 1995. Interaction cloning of Rabin3, a novel protein that associates with the Ras-like GTPase Rab3A. Mol. Cell. Biol. **15:**1137–1143.
11. **Burchard, A. C., R. P. Burchard, and J. A. Kloetzel.** 1977. Intracellular, periodic structures in the gliding bacterium *Myxococcus xanthus*. J. Bacteriol. **132:**666–672.
12. **Cohen, C., and D. A. Parry.** 1990. Alpha-helical coiled coils and bundles: how to design an alpha-helical protein. Proteins **7:**1–15.
13. **Gietz, R. D., B. Triggs-Raine, A. Robbins, K. C. Graham, and R. A. Woods.** 1997. Identification of proteins that interact with a protein of interest: applications of the yeast two-hybrid system. Mol. Cell. Biochem. **172:**67–79.
14. **Haberland, J., J. Becker, and V. Gerke.** 1997. The acidic C-terminal domain of *rna1p* is required for the binding of RanGTP and for RanGAP activity. J. Biol. Chem. **272:**24717–24726.
15. **Hartzell, P., and D. Kaiser.** 1991. Function of MglA, a 22-kilodalton protein essential for gliding in *Myxococcus xanthus*. J. Bacteriol. **173:**7615–7624.
16. **Hodgkin, J., and D. Kaiser.** 1977. Cell-to-cell stimulation of movements in non-motile mutants of *Myxococcus xanthus*. Proc. Natl. Acad. Sci. USA **74:** 2938–2942.
17. **Hodgkin, J., and D. Kaiser.** 1979. Genetics of gliding motility in *Myxococcus xanthus* (*Myxobacterales*): genes controlling movement of single cells. Mol. Gen. Genet. **171:**167–171.
18. **Hodgkin, J., and D. Kaiser.** 1979. Genetics of gliding motility in *Myxococcus xanthus* (*Myxobactererales*): two gene systems control movement. Mol. Gen. Genet. **171:**177–191.
19. **Hong, S., D. R. Zusman, and W. Shi.** 2000. Type IV pilus of *Myxococcus xanthus* is a motility apparatus controlled by the *frz* chemotaxis homologs. Curr. Biol. **10:**1143–1146.
20. **Hurme, R., E. Namork, E. L. Nurmiaho-Lassila, and M. Rhen.** 1994. Intermediate filament-like network formed *in vitro* by a bacterial coiled-coil protein. J. Biol. Chem. **269:**10675–10682.
21. **Ishikawa, J., and K. Hotta.** 1999. FramePlot: a new implementation of the frame analysis for predicting protein-coding regions in bacterial DNA with a high G + C content. FEMS Microbiol. Lett. **174:**251–253.
22. **James, P., J. Halladay, and E. A. Craig.** 1996. Genomic libraries and a host strain designed for highly efficient two-hybrid selection in yeast. Genetics **144:**1425–1436.
23. **Kearns, D. B., P. J. Bonner, D. R. Smith, and L. J. Shimkets.** 2002. An extracellular matrix-associated zinc metalloprotease is required for dilauroyl phosphatidylethanolamine chemotactic excitation in *Myxococcus xanthus*. J. Bacteriol. **184:**1678–1684.
24. **Kroos, L., and D. Kaiser.** 1987. Expression of many developmentally regulated genes in Myxococcus depends on a sequence of cell interactions. Genes Dev. **1:**840–854.
25. **Lazzaroni, J. C., P. Germon, M. C. Ray, and A. Vianney.** 1999. The Tol proteins of *Escherichia coli* and their involvement in the uptake of biomolecules and outer membrane stability. FEMS Microbiol. Lett. **15:**191–197.
26. **MacRae, T. H., and D. McCurdy.** 1976. Evidence for motility-related fimbriae in the gliding microorganism *Myxococcus xanthus*. Can. J. Microbiol. **22:**1589–1593.
27. **Martin, S., E. Sodergren, T. Masuda, and D. Kaiser.** 1978. Systematic isolation of transducing phages for *Myxococcus xanthus*. Virology **88:**44–53.
28. **Matsumura, P., J. J. Rydel, R. Linzmeier, and D. Vacante.** 1984. Overexpression and sequence of the *Escherichia coli cheY* gene and biochemical activities of the CheY protein. J. Bacteriol. **160:**36–41.
29. **Oas, T. G., L. P. McIntosh, E. K. O'Shea, F. W. Dahlquist, and P. S. Kim.** 1990. Secondary structure of a leucine zipper determined by nuclear magnetic resonance spectroscopy. Biochemistry **29:**2891–2894.
30. **Ohba, T., M. Ishino, H. Aoto, and T. Sasaki.** 1998. Dot far-western blot analysis of relative binding affinities of the Src homology 3 domains of Efs and its related proteins. Anal. Biochem. **262:**185–192.
31. **O'Shea, E. K., R. Rutkowski, and P. S. Kim.** 1989. Evidence that the leucine zipper is a coiled coil. Science **243:**538–542.
32. **Sambrook, J., E. F. Fritsch, and T. Maniatis.** 1989. Molecular cloning: a laboratory manual, 2nd ed. Cold Spring Harbor Laboratory Press, Cold Spring Harbor, N.Y.
33. **Schmidt-Lorenz, W.** 1969. The fine structure of the swarm cells of myxobacteria. J. Appl. Bacteriol. **32:**22–23.
34. **Shi, W., and D. R. Zusman.** 1993. The two motility systems of *Myxococcus xanthus* show different selective advantages on various surfaces. Proc. Natl. Acad. Sci. USA **90:**3378–3382.
35. **Skare, J. T., B. M. Ahmer, C. L. Seachord, R. P. Darveau, and K. Postle.** 1993. Energy transduction between membranes. TonB, a cytoplasmic membrane protein, can be chemically cross-linked in vivo to the outer membrane receptor FepA. J. Biol. Chem. **268:**16302–16308.
36. **Spormann, A. M., and D. Kaiser.** 1999. Gliding mutants of *Myxococcus xanthus* with high reversal frequencies and small displacements. J. Bacteriol. **181:**2593–2601.
37. **Spratt, B. G., P. J. Hedge, S. T. Heesey, A. Edelman, and J. K. Broome-Smith.** 1986. Kanamycin-resistant vectors that are analogues of pUC8, pUC9, pEMBL8 and pEMBL9. Gene **41:**337–342.
38. **Stephens, K., P. L. Hartzell, and D. Kaiser.** 1989. Gliding motility in *Myxococcus xanthus*: *mgl* locus, RNA, and predicted protein products. J. Bacteriol. **171:**819–830.
39. **Thomasson, B., J. Link, A. G. Stassinopoulos, N. Burke, L. Plamann, and P. L. Hartzell.** 2002. The GTPase, MglA, interacts with a tyrosine kinase to control type-IV pili-mediated motility of *Myxococcus xanthus*. Mol. Microbiol. **46:**1399–1413.
40. **Ueki, T., S. Inouye, and M. Inouye.** 1996. Positive-negative KG cassettes for construction of multi-gene deletions using a single drug marker. Gene **183:** 153–157.
41. **Wall, D., P. E. Kolenbrander, and D. Kaiser.** 1999. The *Myxococcus xanthus pilQ* (*sglA*) gene encodes a secretin homolog required for type IV pilus biogenesis, social motility, and development. J. Bacteriol. **181:**24–33.
42. **Ward, M. J., H. Lew, and D. R. Zusman.** 2000. Social motility in *Myxococcus xanthus* requires FrzS, a protein with an extensive coiled-coil domain. Mol. Microbiol. **37:**1357–1371.
43. **Weimer, R. M., C. Creighton, A. Stassinopoulos, P. Youderian, and P. L. Hartzell.** 1998. A chaperone in the HSP70 family controls production of extracellular fibrils in *Myxococcus xanthus*. J. Bacteriol. **180:**5357–5368.
44. **White, D. J., and P. L. Hartzell.** 2000. AglU, a protein required for gliding motility and spore maturation of *Myxococcus xanthus*, is related to WD-repeat proteins. Mol. Microbiol. **36:**662–678.
45. **Wolf, E., P. S. Kim, and B. Berger.** 1997. MultiCoil: a program for predicting two- and three-stranded coiled coils. Protein Sci. **6:**1179–1189.
46. **Wolgemuth, C., E. Hoiczyk, D. Kaiser, and G. Oster.** 2002. How myxobacteria glide. Curr. Biol. **12:**369–377.
47. **Wu, S. S., and D. Kaiser.** 1995. Genetic and functional evidence that type IV pili are required for social gliding motility in *Myxococcus xanthus*. Mol. Microbiol. **18:**547–558.
48. **Wu, S. S., and D. Kaiser.** 1997. Regulation of expression of the *pilA* gene in *Myxococcus xanthus*. J. Bacteriol. **179:**7748–7758.
49. **Wurtzel, E. T., M. Y. Chou, and M. Inouye.** 1982. Osmoregulation of gene expression. I. DNA sequence of the *ompR* gene of the *ompB* operon of *Escherichia coli* and characterization of its gene product. J. Biol. Chem. **257:** 13685–13691.
50. **Yanisch-Perron, C., J. Cieira, and J. Messing.** 1985. Improved M13 phage cloning vectors and host strains: nucleotide sequences of the M13mp18 and pUC19 vectors. Gene **33:**103–119.
51. **Youderian, P., N. Burke, D. J. White, and P. L. Hartzell.** 2003. Identification of genes required for adventurous gliding motility in *Myxococcus xanthus* with the transposable element mariner. Mol. Microbiol. **49:**555–570.
52. **Zahrt, T. C., C. Wozniak, D. Jones, and A. Trevett.** 2003. Functional analysis of the *Mycobacterium tuberculosis* MprAB two-component signal transduction system. Infect. Immun. **71:**6962–6970.